Shift and broadening of sodium nS-3P and mD-3P transitions in high pressure NaCd and NaHg discharges

Mioković, Željka; Balković, Darko; Veža, Damir

ISSN 1330–0008
CODEN FIZAE4

SHIFT AND BROADENING OF SODIUM nS–3P AND mD–3P TRANSITIONS IN HIGH PRESSURE NaCd AND NaHg DISCHARGES

ŽELJKA MIOKOVIĆ [a,b], DARKO BALKOVIĆ [a] and DAMIR VEŽA [a,1]

[a] *Physics Department, Faculty of Science, University of Zagreb, Bijenička 32 HR-10 002 Zagreb, Croatia*

[b] *Faculty of Electrical Engineering, University of Osijek, K. Trpimira 2B 31 000 Osijek, Croatia*

[1] *E-mail address: veza@phy.hr*

Dedicated to the memory of Professor Vladimir Šips

Received 1 February 2005; revised manuscript received 3 June 2005
Accepted 13 June 2005 Online 4 December 2005

We report measurements of the Stark shift and Stark width of sodium spectral lines corresponding to $n^2\mathrm{S}_{1/2}$–$3^2\mathrm{P}_{3/2,1/2}$ ($n = 5, 6, 7$) and $m^2\mathrm{D}_{5/2,3/2}$–$3^2\mathrm{P}_{3/2,1/2}$ ($m = 5, 6$) transitions. Measurements have been made on AC-driven high-pressure Na-Hg-Xe and Na-Cd-Xe discharges. Electron density has been determined from the measurements of the Stark shift of sodium $7^2\mathrm{S}_{1/2}$–$3^2\mathrm{P}_{1/2,3/2}$ spectral line. The electron temperature and the density of neutral particles have been determined analyzing the shape of the measured sodium atomic lines, by comparison of the calculated and the observed line profiles. Electron density and temperature range from 6×10^{21} to $1 \times 10^{22}\,\mathrm{m}^{-3}$ and from 3800 to 4100 K, respectively. Dependence of measured Stark shifts and Stark widths on electron density and temperature have been investigated. The final results have been compared with available theoretical and experimental data.

PACS numbers: 52.70.Kz, 52.80.Mg, 52.25.Os UDC 537.228.5
Keywords: Stark shift and width, Na spectral lines, Na-Hg-Xe and Na-Cd-Xe discharges

1. Introduction

The high-pressure sodium-mercury vapour discharge lamp was invented 40 years ago [1], and further developed and refined during the next two decades [2]. It is

a wall-stabilized electric arc burning at elevated pressure and high temperature in mercury-sodium plasma. The lamp burner is made of a high-density polycrystalline alumina ceramics (PCA), a material highly resistant to hot and corrosive sodium vapour up to 1800 K. Despite of its high transmission coefficient ($> 90\%$ for visible radiation), a disadvantage of PCA is that it is not transparent but translucent material.

Optical and electrical features of the high-pressure sodium discharge lamp based on the standard sodium–mercury–xenon filling, have been widely investigated [2]. A similar discharge, based on sodium–cadmium–xenon filling, has been studied so far in order to find out origin of continuous bands in visible part of the spectrum of NaHg, KHg and NaCd molecules [3,4], but plasma parameters of NaCd discharge have been rarely investigated [5]. Yet, these data are desirable for a more complete understanding of the physics and chemistry of all high-pressure discharges containing sodium and IIB group elements (Zn, Cd, Hg). This general knowledge about plasma generated in a vapour mixture of sodium and IIB group elements is important for a possible upgrade to an environmentally-friendly high-pressure mercury-free discharge lamp based on the sodium–zinc filling [6]. Attractive candidates for the determination of electron density and temperature in such plasmas are higher-lying sodium excited states (belonging to nS and mD series) with large Stark shifts and Stark widths and small oscillator strengths. Theoretical Stark-broadening data on sodium m^2D–3^2P and n^2S–3^2P transitions are given by the Griem's [7,8] and Dimitrijević and Sahal-Bréchot [9] calculations. Experimental data are rather scarce. According to our knowledge, there is an older measurement of electron density in Na–Hg–Xe discharge using Stark shifts of 5^2S–3^2P, 4^2D–3^2P and 5^2D–3^2P transitions [10]. Just recently, new measurements of the shifts of 7^2S–3^2P, 5^2D–3^2P and 6^2D–3^2P spectral lines in a Na–Ar pulsed discharge have been published [11]. The accompanying calculations of these line shifts [11] made in the random-phase approximation (RPA) agree with existing Stark-shift calculations [7 – 9]. Mutual agreement between theories [9] and [11], and experiment [11] is especially good in the case of the 7^2S–3^2P transition, suggesting that this line is a very good choice for electron density measurements in all discharges containing sodium as an additive.

In this paper we report the measurements of the Stark shift and Stark width of sodium spectral lines corresponding to n^2S–3^2P ($n = 5, 6, 7$) and m^2D–3^2P ($m = 5, 6$) transitions, originating in NaCd and NaHg high-pressure discharges. Because of the very good agreement between theory and experiment in the case of the $7^2S_{1/2}$–$3^2P_{1/2,3/2}$ line [11], we used this line as a calibration line, i.e. the electron density has been determined from the measurements of the Stark shift of this spectral line. We investigated the dependence of the Stark shift and Stark width of the sodium nS–3P ($n = 5, 6$) and nD–3P ($n = 5, 6$) atomic lines on electron density. The measured data are compared with the available experimental [10,11] and theoretical data [7–9,11]. The observed line shapes are compared with the calculated line shapes obtained using Bartels' method [12].

2. Line-shape calculations

2.1. Broadening mechanisms

The spectral line profiles of sodium nS–3P and mD–3P transitions radiated by excited sodium atoms in a high-pressure arc discharge are influenced by two main broadening mechanisms: the Stark broadening (by electrons) and the van der Waals broadening (by dissimilar atoms) [7,13]. The resonance broadening (by similar atoms) and the Doppler broadening are practically negligible under our experimental conditions [7,14]. The dominant shift and broadening mechanism in this experiment is the Stark broadening by electrons, as it will be justified later.

The shape of an atomic line can be calculated in two different approximations, impact and quasistatic, corresponding to two different interaction pictures. The application of the impact or the quasistatic approximations yields very different line shapes [7]. The *quasistatic approximation* yields the line profile which is due to collisions of the radiating atom with neutral dissimilar atoms (the van der Waals interaction [14,8])

$$P_{\mathrm{QS}}(\Delta\lambda) = \frac{\sqrt{\Delta\lambda_0}}{2\Delta\lambda^{3/2}} \exp\left(- \frac{\pi\Delta\lambda_0}{4\Delta\lambda}\right), \tag{1}$$

where $\Delta\lambda > 0$. This profile yields a broadening of the red wing of sodium lines, and there is no contribution in the blue wing: $P_{\mathrm{QS}}(\Delta\lambda \leq 0) = 0$. The characteristic width of this profile, $\Delta\lambda_0$, and the displacement of its maximum $\delta\lambda_{\max}$ are given as

$$\Delta\lambda_0 = \frac{\lambda_0^2}{2\pi c}\left(\frac{4\pi}{3}\right)^2 C_6^{\mathrm{NaX}} N_{\mathrm{X}}^2, \tag{2}$$

$$\delta\lambda_{\max} = \frac{\lambda_0^2}{2\pi c}\frac{\pi}{6}\left(\frac{4\pi}{3}\right)^2 C_6^{\mathrm{NaX}} N_{\mathrm{X}}^2. \tag{3}$$

Here λ_0 represents the transition wavelength, C_6^{NaX} represents the effective Na–X interaction constant, and X denotes cadmium or mercury atom. The effective C_6^{NaX} interaction constants depend linearly on the perturber (Cd or Hg) dipole polarizability α_{X} [15,16] as $C_6^{\mathrm{NaX}} = \alpha_{\mathrm{X}} e^2(\langle r_i^2\rangle - \langle r_f^2\rangle)$, where $\langle r_i^2\rangle$ and $\langle r_f^2\rangle$ are the mean square radii of the valence electron in the initial and the final excited sodium state [14].

On the other hand, the *impact approximation* yields the Lorentzian line shape regardless of the broadening mechanism (in our case Stark and van der Waals broadening) [7]

$$P_{\mathrm{L}}(\Delta\lambda) = \frac{\Delta\lambda_{1/2}}{2\pi}\frac{1}{(\Delta\lambda - \delta\lambda_{1/2})^2 + (\Delta\lambda_{1/2}/2)^2}, \tag{4}$$

where $\delta\lambda_{1/2}$ is the line shift, and $\Delta\lambda_{1/2}$ is the full width at half maximum (FWHM) of the Lorentzian profile. The line width and the line shift of the Lorentzian profile in

this case are due to Stark and van der Waals interactions [2,7]. The total line width is given by the sum of the Stark and van der Waals line widths, $\Delta\lambda_{1/2} = (\Delta\lambda_{1/2})_{\rm S} + (\Delta\lambda_{1/2})_{\rm vdW}$. The total line shift is given by $\delta\lambda_{1/2} = (\delta\lambda_{1/2})_{\rm S} + (\delta\lambda_{1/2})_{\rm vdW}$, the sum of the Stark and van der Waals line shifts [7,8,14].

Quantum-mechanical calculations [7] lead to the following dependence of the FWHM of a Stark broadened line and its shift on electron density

$$\big(\Delta\lambda_{1/2}\big)_{\rm S} = 2\big[1 + 1.75A(1 - 0.75R)\big]w_{\rm e}N_{\rm e}, \tag{5}$$

$$\big(\delta\lambda_{1/2}\big)_{\rm S} = \left[\frac{d_{\rm e}}{w_{\rm e}} \pm 2A\,(1 - 0.75R)\right]w_{\rm e}N_{\rm e}. \tag{6}$$

The Stark half-halfwidth data ($w_{\rm e}$ values) and Stark-shift data ($d_{\rm e}$ values) due to electron broadening, as well as the ion broadening parameter A, are tabulated in Refs. [7], [8] and [9] for a reference electron density of $10^{22}\,{\rm m}^{-3}$ and a broad temperature range. Parameter R represents the ratio of the mean distance between ions and the Debye radius [7],

$$R = \frac{r_1}{\rho_{\rm D}} = 6^{1/3}\pi^{1/6}\left(\frac{e^2}{4\pi\varepsilon_0 k_{\rm B}T_{\rm e}}\right)^{1/2} N_{\rm e}^{1/6}. \tag{7}$$

A line broadened by the van der Waals interaction has, according to the Lindholm–Foley impact theory, the FWHM, $(\Delta\lambda_{1/2})_{\rm vdW}$, and the line shift, $(\delta\lambda_{1/2})_{\rm vdW}$, given by [14]

$$\big(\Delta\lambda_{1/2}\big)_{\rm vdW} = 8.08\frac{\lambda_0^2}{2\pi c}\big(C_6^{{\rm Na}X}\big)^{2/5} v^{3/5} N_X, \tag{8}$$

$$\big(\delta\lambda_{1/2}\big)_{\rm vdW} = 2.94\frac{\lambda_0^2}{2\pi c}\big(C_6^{{\rm Na}X}\big)^{2/5} v^{3/5} N_X. \tag{9}$$

Here v is the relative velocity of interacting atoms, $C_6^{\rm NaX}$ represents the effective Na–X interaction constant, and X stands for the perturbing atoms (Cd or Hg). The $C_6^{{\rm Na}X}$ interaction constants are calculated using the data given in Refs. [15–17].

According to Kielkopf [18] and Stormberg [13], the total line profile can be successfully simulated by convoluting the impact line profile and the quasistatic line profile

$$P_{\rm T}(\Delta\lambda) = \int P_{\rm L}(\Delta\lambda - \zeta)P_{\rm QS}(\zeta){\rm d}\zeta. \tag{10}$$

The convolution integral gives a line profile expressed in a complicated but analytical form that can be rapidly calculated [19]. This empirical approach has been suggested long time ago by Margenau [20], Hindmarsh et al. [21], Kielkopf et al. [18], and recently by Stormberg [13]. The resultant synthetic line profile describes simultaneously the line core and the line wings. However, whereas this approach

is mathematically correct, it can be questioned from the physical point of view. It suggests that we can convolute two broadening mechanisms that are strictly limited: one to the line core (giving the impact line profile), and the other one to the line wing (delivering the quasistatic line profile). However, justification for the application of this synthetic profile and its popularity in line shape analysis [8,22 – 24], comes from the fact that it smoothly and correctly describes the complete line shape, behaving as a Lorentzian in the line core and in the blue line wing, and as an exponential in the red line wing. After Stormberg [13], several authors successfully applied this approach to the analysis of the shape of atomic lines radiated by various high-pressure discharges (sodium lines in high-pressure sodium and metal-halide discharges [16,22,23], and mercury lines in high-pressure mercury discharge [24]). In this work, the line profiles were calculated by the line shape function $P_{\mathrm{T}}(\Delta\lambda)$ and the synthetic line shape was used in the Bartels' method to obtain the true line shape emitted by the discharge.

2.2. Bartels' method

This method [25] is based on the assumptions that the axially-symmetric plasma is in local thermodynamic equilibrium (LTE), the equation of state for ideal gas is valid, the partial pressure of the emitting atoms is constant throughout the plasma column, and that the depletion of the ground state population due to excitation and ionisation can be neglected. The population of an excited atomic state is then given by the Boltzmann equation

$$N_n(r) = N_0(r)\frac{g_n}{g_0}\exp\left(-\frac{E_n}{k_{\mathrm{B}}T(r)}\right), \tag{11}$$

where g_n and g_0 are the statistical weights of the level n and of the ground state, respectively. The ground-state atomic density, $N_0(r)$, is related to the total vapour pressure and the gas temperature via the equation of state

$$N_0(r) = \frac{g_0}{U(T)}\ \frac{p}{k_{\mathrm{B}}T(r)}, \tag{12}$$

where $U(T)$ is the partition function of the atom, k_{B} is the Boltzmann constant and p is the local vapour pressure. Under the high-pressure discharge conditions, the partition function $U(T)$ is approximately equal to g_0. $T(r)$ is the assumed temperature distribution along a radius of the discharge

$$T(r) = T_{\mathrm{A}} - \left(T_{\mathrm{A}} - T_{\mathrm{W}}\right)\left(\frac{r}{R}\right)^n, \tag{13}$$

where T_{A} is the axis temperature, T_{W} is the wall temperature, and $n \cong 2$ (a parabolic temperature distribution).

Finally, the intensity of a spectral line within Bartels' method is given by

$$I(\nu) = \frac{2h\nu^3}{c^2}\exp\left(-\frac{h\nu}{k_{\mathrm{B}}T}\right)MY(\tau_0, p), \tag{14}$$

where τ_0 is the optical depth, and the function $Y(\tau_0, p)$ represents the influence of the optical depth on the peak-line intensity (it could be expressed parametrically). The parameters M and p describe the inhomogeneity of the plasmas, so that $p = 1$ corresponds to a homogeneous plasma column and $p = 0$ to a completely inhomogeneous source. The energy of the lower level for the line under investigation must satisfy the conditions $k_{\mathrm{B}}T \ll E_n$ (pressure-broadening case) and $k_{\mathrm{B}}T \ll E_n + 0.5E_{\mathrm{i}}$ (Stark-broadening case). The function M must satisfy conditions $M = \sqrt{E_n/E_m}$ (van der Waals broadening) and $M = \sqrt{E_n + 0.5E_{\mathrm{i}}}/\sqrt{E_m + 0.5E_{\mathrm{i}}}$ (Stark broadening). E_n and E_m are the energies of the lower and the upper level of the atomic line, respectively, whereas E_{i} is the ionisation energy. Both, M and p, are constant within a spectral line.

3. *Experimental setup*

The experimental arrangement is shown in Fig. 1. The measurements were performed using a 400 W NaCd and NaHg high-pressure discharges (with translucent sapphire burner) in series with a 400 W inductive choke. The inner diameter, the outer diameter and the length of the sapphire burner are 7.6 mm, 9 mm and 110 mm, respectively. The tips of the electrodes are separated 95 mm. The discharge was operated vertically, driven by a standard 50 Hz AC line source, with a discharge current between 3 A and 4.2 A for the NaCd, and between 2.6 A and 4 A for the NaHg high-pressure lamp. The burner contains a sodium–cadmium (or sodium–mercury) amalgam. Partial pressure of sodium and cadmium (or mercury) during lamp operation is determined by the temperature of the coldest spot of the burner [26]. The central region of the burner was imaged onto the entrance

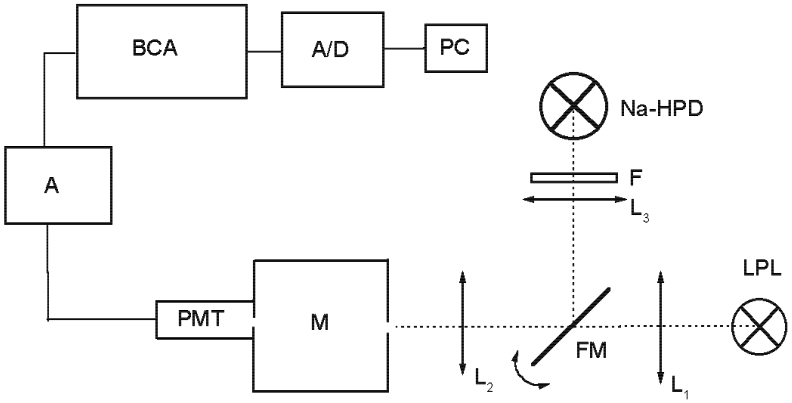

Fig. 1. The experimental arrangement: HPD - high pressure sodium discharge, LPL - low pressure sodium lamp, F - cut off filter, L - lens, FM - folding mirror, M - monochromator, PMT - photomultiplier, A - linear amplifier, BCA - box car averager, A/D - analog to digital converter, PC - personal computer.

slit of a medium-resolution monochromator (Karl Zeiss, Model SPM-2, 10 μm wide slits). The magnification ratio was approximately 1:1. The light from the discharge, spectrally resolved by the monochromator, was detected using an EMI 9558QB photomultiplier. A linear amplifier (Keithley electrometer, M611) with a low-pass electronic filter for the suppression of high-frequency noise has been used for signal amplification.

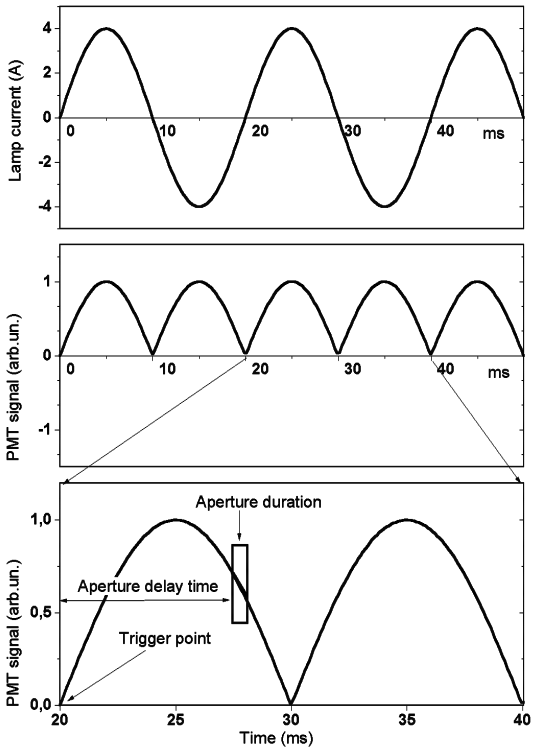

Fig. 2. An illustration of the measurement process. The upper part of the figure displays the AC discharge current, the middle part - the corresponding time dependence of the photomultiplier signal, and the lower part - a general case of timing for data acquisition. In our experiments the data are sampled at the current maximum (5 ms *aperture delay time) and with the 50* μs *aperture duration.*

The signals were processed by a box-car averager equipped with a gated integrator, operated either in external or in-line triggering mode as illustrated in Fig. 2. The current reversal point is the reference time instant and the origin of the trigger. The trigger signal can be derived either by monitoring the integral light signal by a photodiode, or by monitoring the AC current. This technique allows sampling out the spectrum of plasma radiation at any desirable phase of the AC current. In this experiment, we performed all measurements using the aperture duration time of 50 μs, and the aperture delay time of 5 ms (at the current maximum). The processed data have been converted by a 14-bit A/D converter, and stored in a computer for further analysis.

Calibration of the monochromator wavelength scale is provided by low-pressure sodium and mercury lamps, since the shift of spectral lines radiated by the low-pressure plasma can be neglected.

4. Plasma diagnostics and reduction of data

To allow comparison of our data with the results of earlier experiments [10,11] and with the calculations of Stark widths and Stark shifts made under assumption of LTE [7–9,11], we have to check validity of LTE approximation in our AC driven arc discharge. Here we will show that our discharge satisfies all validity criteria for the assumption of LTE, and that the data may be compared to data measured in previous experiments.

In Ref. [10], the authors describe the measurements of Stark widths and Stark shifts of 5^2S–3^2P and 5^2D–3^2P emission lines from a NaHg arc, burning in a tube made of clear sapphire (electrode separation 8.6 cm, internal diameter 7.6 mm). The arc was operated with a switching DC power source, with the 80 ms switching time. The measured electron densities in the core of the arc were about 1×10^{21} m^{-3}, justifying the assumption of LTE. In recent experiment [11] authors measured Stark shifts on 7^2S–3^2P, 5^2D–3^2P and 6^2D–3^2P lines from a Na–Ar arc burning in a clear sapphire tube (electrode separation 7.6 cm, internal diameter 4.8 mm). The arc was operated in a simmer-mode, powered with rectangular current pulses of 1 ms duration [11]. Electron densities in the core of the arc were measured as high as 1×10^{23} m^{-3}, justifying also the assumption of LTE. The electron density range, the core arc temperature and the density of neutral atoms in these discharges are very similar to our experimental conditions.

A comprehensive discussion of the validity criteria for the assumption of LTE can be found in Ref. [7]. In the case of a stationary plasma, for complete LTE down to the ground state, the collision excitation rate must be much larger than the radiative excitation or de-excitation rate, even for the first excited state. Since the resonance lines of the main discharge constituent (neutral mercury or cadmium) are self-absorbed, the condition for validity of LTE requires (Eq. 6.60 in Ref. [7])

$$N_\mathrm{e} \geq 9 \times 10^{17} \sqrt{\frac{k_\mathrm{B}T}{E_H}} \left(\frac{E_2 - E_1}{E_H} \right)^3 , \tag{15}$$

where the symbols have the same meaning as in Ref. [7]. This condition requires rather high electron densities, but it can be reduced by an order of magnitude if the product of the ground state atom density, N_1, and the discharge diameter, d, is large enough (Eq. 6.64 in Ref. [7]),

$$N_1 d \geq 4 \times 10^9 f_{12}^{-1} \lambda_{12}^{-1} \sqrt{\frac{k_\mathrm{B}T}{AE_H}} , \tag{16}$$

where f_{12} denotes the resonance line oscillator strength, λ_{12} is the wavelength of the line, and A represents the relative atomic mass number. Since Eq. (16) is satisfied in our experiments, Eq. (15) may be safely relaxed by an order of magnitude, to the relation

$$N_\mathrm{e} \geq 10^{17} \sqrt{\frac{k_\mathrm{B}T}{E_H}} \left(\frac{E_2 - E_1}{E_H} \right)^3 , \tag{17}$$

which for neutral mercury or cadmium (the most stringent requirement) becomes $N_\mathrm{e} > 7 \times 10^{20}\,\mathrm{m}^{-3}$. This basic requirement for the validity of LTE is always satisfied in our measurements since in all experiments, the line widths and shifts are determined at $N_\mathrm{e} \geq 1 \times 10^{21}\,\mathrm{m}^{-3}$. However, to prove the validity of LTE, one must additionally check whether the kinetic temperatures of atoms and ions are equal to the electron temperature. This condition is given as (Eq. 6.75 in Ref. [7])

$$E^2 \ll \left(5.5 \times 10^{-12} N_\mathrm{e} \frac{E_H}{k_\mathrm{B} T}\right)^2 \frac{m}{M}, \tag{18}$$

where E is the applied electric field, and the other symbols have the same meaning as in Ref. [7]. Since this condition is satisfied, we can expect that the temperatures of heavy particles were equal to the electron temperature to within $\pm 2\%$ [7].

Since our discharge is AC operated, and data are sampled at each current maximum point with the 50 μs aperture duration (see Fig. 2), we also have to check the validity of LTE in the case of time-dependent plasmas. Theory requires that the time necessary for the equilibration between atomic states be less then a typical time for a 10% variation in plasma conditions during the period in which we make the measurement. The time required for the equilibration between the states with quantum numbers n and $n+1$ is given as (Eq. 6.67 in Ref. [7])

$$t \geq t_\mathrm{crit}, \quad t_\mathrm{crit} = \frac{4.5 \times 10^7}{n^4 N_\mathrm{e}} \sqrt{\frac{k_\mathrm{B} T}{E_H}} \exp\left(\frac{E_{n+1} - E_n}{E_H}\right), \tag{19}$$

where the symbols have the meaning as in Ref. [7]. For the ground state and the first excited state of neutral Hg or Cd (the most stringent requirement), this formula yields $t_\mathrm{crit} = 60$ μs. Since typical time allowed for plasma variation in our experiment is 50 μs (aperture duration time), this condition is barely satisfied for resonance levels of neutral mercury (or cadmium), but it is entirely satisfied for all higher atomic states of all constituents of our plasmas.

Finally, we have to check the conditions of validity of the isolated-line approximation [7] for the sodium lines of interest. Generally, at lower electron densities, the line shifts due to the quadratic Stark effect, are proportional to the electron density. Experiments in dense plasmas, made at higher electron densities, show deviations from this linear behaviour. The determination of the electron density at which the deviation from linearity can start is very important since it establishes range of validity of the isolated-line approximation. By definition [7,9], a line can be regarded as isolated if its initial and final (non-degenerate) energy levels E_i and E_f, broadened by electron collisions, do not overlap, i.e. if $2w_\mathrm{e}^i \leq \omega_{in}$ and $2w_\mathrm{e}^f \leq \omega_{fm}$. Here $2w_\mathrm{e}^i$ and $2w_\mathrm{e}^f$ are the corresponding level widths, and ω_{in} (or ω_{fm}) is the distance to the corresponding nearest perturbing level, E_n and E_m. To check whether a line is isolated, we can use parameter $C = 2w_\mathrm{e}/(\Delta E_{ij})_\mathrm{min}$ listed in Ref. [9] for each sodium line. The corresponding "critical" electron density, N_l, can be expressed as $N_l = C/2w_\mathrm{e}$, where w_e is the line half-width at the reference electron density of $1 \times 10^{22}\,\mathrm{m}^{-3}$. It can be easily checked that for all nS–3P lines, departure from linear behavior can be expected at very high electron densities ($N_l \geq 1 \times 10^{23}\,m^{-3}$). This

suggests that all nS–3P lines can be safely treated as isolated in the electron density range used in our experiments. On the contrary, the value of the critical electron density for the 5D–3P line it is only about $1 \times 10^{22}\,\mathrm{m}^{-3}$, and for the 6D–3P line it is even lower, $4 \times 10^{21}\,\mathrm{m}^{-3}$, suggesting that these two lines could not be regarded as completely isolated.

In the case of n^2S–3^2P ($n = 5, 6, 7$) and m^2D–3^2P ($m = 5, 6$) sodium lines, and in the discharge parameter range of interest (3800 K $\leq T_\mathrm{e} \leq$ 4100 K, $6 \times 10^{21} < N_\mathrm{e} < 1 \times 10^{22}\,\mathrm{m}^{-3}$, $1 \times 10^{23} < N_\mathrm{Na} < 4 \times 10^{23}\,\mathrm{m}^{-3}$, $5 \times 10^{23} < N_\mathrm{X} < 2.5 \times 10^{24}\,\mathrm{m}^{-3}$, where X stands for Cd and Hg, the Stark broadening dominates over van der Waals broadening. That statement can be proved by inserting appropriate interaction constants, plasma parameters and other experimental data in Eqs. (2)–(11). To demonstrate it, we can use the data on the 6S–3P line measured in NaHg and NaCd discharges at an electron density of $9 \times 10^{15}\,\mathrm{cm}^{-3}$. The corresponding discharge temperature is determined to be 3800 K in NaHg and 3900 K in NaCd discharge. The mean relative velocity of the Na–Hg (or Na–Cd) atomic pairs at this temperature is about $2 \times 10^3\,\mathrm{m/s}$. An average density of the ground-state mercury (or cadmium) atoms at this temperature is about $2 \times 10^{24}\,\mathrm{m}^{-3}$, and an average ground state sodium-atom density is about $3 \times 10^{23}\,\mathrm{m}^{-3}$. The static polarizability of mercury atoms is 34.4 a.u., and 49.7 a.u. for cadmium atoms [15,16]. The corresponding effective C_6 constant for Na*–Hg pair is about $4 \times 10^{-29}\,\mathrm{s}^{-1}\mathrm{cm}^6$, and for Na*–Cd pair is about $5 \times 10^{-29}\,\mathrm{s}^{-1}\mathrm{cm}^6$. These values lead to an impact line shift (caused by Cd or Hg perturbers) of about 0.006 nm, and to a displacement of the maximum of the quasistatic profile of about 0.00025 nm. The corresponding typical line-broadening values are about 0.017 nm for the impact line width, and about 0.0005 nm for the characteristic width of the quasistatic profile. Furthermore, the Na(6S)–Na(3P) interaction, according to the Lindholm–Foley impact theory [14], with a calculated interaction constant of about $2 \times 10^{-10}\,\mathrm{s}^{-1}\mathrm{cm}^3$, delivers a completely negligible line width, and a zero line shift. The Doppler broadening at this temperature contributes about 0.004 nm to the line width, and also causes a null line shift.

At the indicated electron density ($N_\mathrm{e} = 9 \times 10^{15}\,\mathrm{cm}^{-3}$), the measured 6^2S–3^2P total line shifts are about 0.08 nm. Using the plasma parameters indicated above, our fitting procedure delivers a Stark width for this transition of about 0.045 nm. The calculated shift and broadening data for other two n^2S–3^2P and m^2D–3^2P lines are basically very similar. Consequently, the line shifts of all n^2S–3^2P and m^2D–3^2P transitions are heavily dominated by the Stark shift, $\left(\delta\lambda_{1/2}\right)_\mathrm{S} \gg \left(\delta\lambda_{1/2}\right)_\mathrm{vdW}$. The corresponding line widths are significantly dominated by Stark broadening, $\left(\Delta\lambda_{1/2}\right)_\mathrm{S} > \left(\Delta\lambda_{1/2}\right)_\mathrm{vdW}$. Furthermore, since typical ratio of the mean distance between ions and the Debye radius is $R \leq 0.65$ (Eq. (6)), the contribution of ion broadening to the total line width and shift of n^2S–3^2P lines should be less than 10%. Therefore, one can assume for the Stark broadening and shift parameters (Eqs. (5)–(6)) a linear dependence on electron density. On the other hand, the contribution of ion broadening to the total line width and shift of the n^2D–3^2P lines could be up to 25%, and one cannot assume for Stark-broadening parameters a reliable linear dependence on electron density.

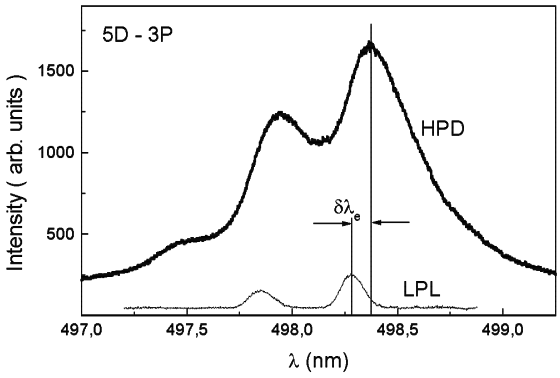

Fig. 3. Determination of the line shifts. The line positions measured in the spectrum of high-pressure sodium discharge and in the spectrum of the low-pressure sodium lamp are compared, yielding the Stark shift $\left(\delta\lambda_{1/2}\right)_{\mathrm{S}}$ *of the corresponding line profile. In this example, measurement of the total line shift,* $\delta\lambda_{\mathrm{e}}$*, of the* 5D–3P *sodium line is illustrated. The small and broad feature (at 497.4* nm*) in the blue wing of the weaker component is a forbidden* Na *line.*

The principle of the measurement of line shifts [26] is shown in Fig. 3. The line positions measured from the high-pressure sodium discharge and from the low-pressure sodium lamp can be directly compared, delivering Stark shift, $\left(\delta\lambda_{1/2}\right)_{\mathrm{S}}$ of the corresponding line profiles. On the contrary, the Stark widths, the discharge temperature and the density of neutrals are determined indirectly, by fitting the synthetic line shapes to the measured line profiles as shown in the Fig. 4. The 6S–3P line shown in this figure is measured in the NaCd discharge at an electron density of $(9\pm2.3)\times10^{21}\,\mathrm{m}^{-3}$. The discharge temperature is determined to be (3900 ± 100) K. The mean relative velocity of the Na–Cd pairs at this temperature is $2.07\times10^{3}\,\mathrm{m/s}$. The density of the ground state cadmium atoms is $(1.8\pm0.6)\times10^{24}\,\mathrm{m}^{-3}$, and the

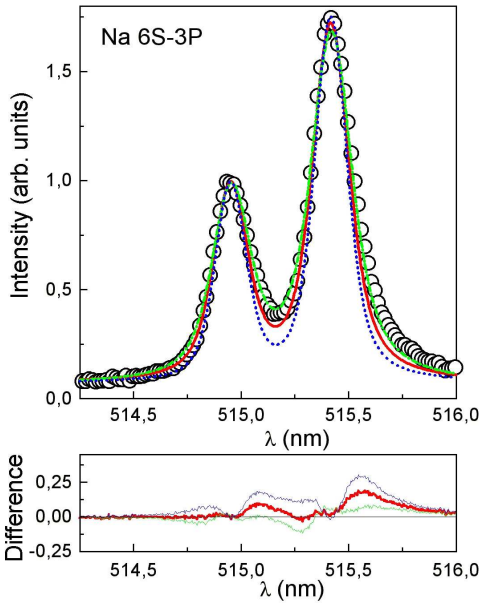

Fig. 4. Determination of the line widths. This line was measured in NaCd *discharge at* $N_{\mathrm{e}}=(9\pm2.3)\times10^{21}\ \mathrm{m}^{-3}$*. Other discharge parameters are:* $T_{\mathrm{e}}=(3900\pm100)$ K, $N_{\mathrm{Cd}}=(1.8\pm0.6)\times10^{24}\,\mathrm{m}^{-3}$, $N_{\mathrm{Na}}=(2.7\pm0.8)\times10^{23}\,\mathrm{m}^{-3}$, *effective* $C_6^{\mathrm{NaCd}}=5.4\times10^{-29}\,\mathrm{s}^{-1}\mathrm{cm}^{6}$*. The line shift of this transition is strongly dominated by the Stark shift,* $\left(\delta\lambda_{1/2}\right)_{\mathrm{S}}\approx15\left(\delta\lambda_{1/2}\right)_{\mathrm{vdW}}$ *(see text for discussion). The full line represents the best fit. The dashed (dotted) line represents the fit with 25% larger (smaller) Stark width. The small picture shows the residuals between corresponding calculated line shape and experimental points.*

ground state sodium atom density is $(2.7\pm0.8)\times10^{23}\,\mathrm{m}^{-3}$. The static polarizability, α, of cadmium atoms is 49.7 a.u. [15]. The corresponding effective C_6 constant for $\mathrm{Na}^*(6\mathrm{S})$–Cd pair is $5.4\times10^{-29}\,\mathrm{s}^{-1}\mathrm{cm}^6$. These values lead to an impact van der Waals line shift of 0.0055 nm, and to a displacement of the quasistatic profile of 0.00022 nm. Corresponding line-broadening values are 0.015 nm for the impact line width, and 0.00043 nm for the characteristic width of the quasistatic profile. At the electron density of $9\times10^{21}\,\mathrm{m}^{-3}$ the total $6^2\mathrm{S}$–$3^2\mathrm{P}$ line shift is measured as (0.08 ± 0.02) nm, and our fitting procedure yields (0.044 ± 0.011) nm as the Stark width of this transition. Since the line shift of $6^2\mathrm{S}$–$3^2\mathrm{P}$ transition is completely dominated by the Stark shift, $\left(\delta\lambda_{1/2}\right)_{\mathrm{S}} \approx 15\left(\delta\lambda_{1/2}\right)_{\mathrm{vdW}}$, the measured total line shift practically corresponds to the Stark shift.

The synthetic line shapes calculated within the Bartels' method were numerically convoluted [27] with the (0.13 ± 0.01) nm wide Gaussian instrumental profile (determined in a separate experiment) in order to obtain the profile that can be directly compared to the measured one. The full line in Fig. 4 represents the best fit. The dashed (dotted) line represents the fit with the 25% larger (smaller) Stark width. The lower picture shows the difference between the calculated line shapes and the experimental line shape. Note that the best profile fit almost exactly fits the blue wing of the weaker component, and also fits very well the blue wing of the stronger component. Both components show a slight residual discrepancy between the calculated and the measured red-line wing (about 8% difference in the red wing). We strongly believe that this residual line shape discrepancy is caused by the quasistatic ion broadening.

5. *Results and discussion*

In Figs. 5a – c, results of our measurements of line shifts of the nS–3P lines ($n = 5, 6, 7$) are compared with the available theoretical data [7 – 9]. Note that electron densities in the NaCd and NaHg discharges are derived from the shift data of the 7S–3P line (Fig. 5(a)) with the Stark broadening parameters calculated from Refs. [9] and [11]. Traditionally, the line-shift data are regarded as less reliable for the determination of electron density in a discharge because of the difficulties in making accurate theoretical predictions. Since several contributions of different sign could be responsible for the Stark shift of spectral lines, the theoretical shift parameters usually have a larger uncertainty. Fortunately, in the case of the 7S–3P transition, two main contributions to the line shift stem form the interaction with the 7P and 6P levels, and lead to the shifts of opposite sign [11]. They change energy of the 7S level by about -0.085 eV and $+0.062$ eV, respectively. In addition, their sum is almost linear with respect to the electron density. The random-phase (RPA) calculations of the 7S–3P line shift [11] completely confirm the line-shift data of Dimitrijević and Sahal-Bréchot [9]. Apparently, the 7S–3P line is well suited to measure electron density in high-pressure discharges containing sodium in the range of electron densities up to $10^{23}\,\mathrm{m}^{-3}$. Consequently, our experimental points of the measured shift data for the 7S–3P line are placed exactly on the line given by the theoretical

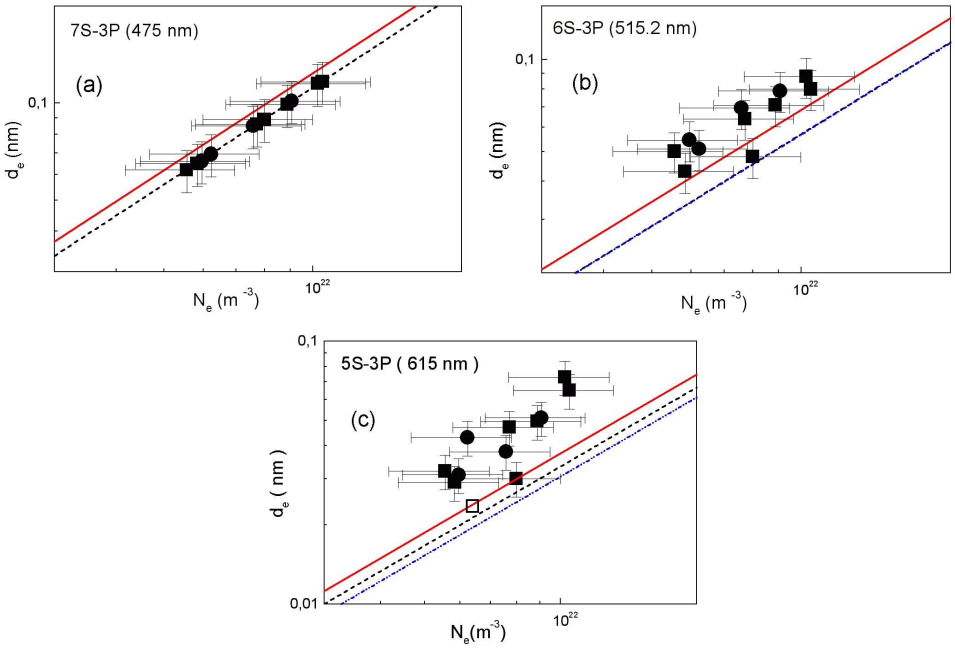

Fig. 5. Results of measurements of the Stark shifts. Explanation of the symbols: filled squares - this experiment, NaHg *discharge; filled circles - this experiment,* NaCd *discharge; dashed line - theory [9]; solid line - theory [7]; The results are given: a) for the* 7S–3P *transition; this line was used as the calibration line for other measurements, b) for the* 6S–3P *transition; this panel also includes the results of calculations of Griem [8] (dot-dashed line) which practically coincide with the results of Dimitrijević [9], and c) for the* 5S–3P *transition; this panel also includes experimental results of Ref. [10] (open squares) and the results of calculations of Griem [8] (dot-dashed line). Our estimated experimental error is* $\pm 25\%$*. Claimed uncertainty of calculated shifts is about 30% [7].*

calculations of Dimitrijević and Sahal-Bréchot [9]. However, one can note that calculations both in Refs. [7] and [9] are within our experimental error bars ($\pm 25\%$). In addition, one should take into account that claimed uncertainty of calculated shift data is about 30% [7]. The 6S–3P and the 5S–3P lines show a small but systematic discrepancy between experiment and calculations.

In Figs. 6a – c, results of our determinations of line widths of the nS–3P lines ($n = 5, 6, 7$) are compared with the available theoretical data [7–9]. The experimental points of the Stark-width data for the 7S–3P line are scattered around the calculated values of Dimitrijević and Sahal-Bréchot [9]. However, note again that both calculations, in Refs. [7] and [9], are within our experimental error bars ($\pm 25\%$), and that claimed uncertainty of calculated width data is about 30% [7]. The widths of the 6S–3P and the 5S–3P lines show a small but systematic discrepancy between experiment and calculations.

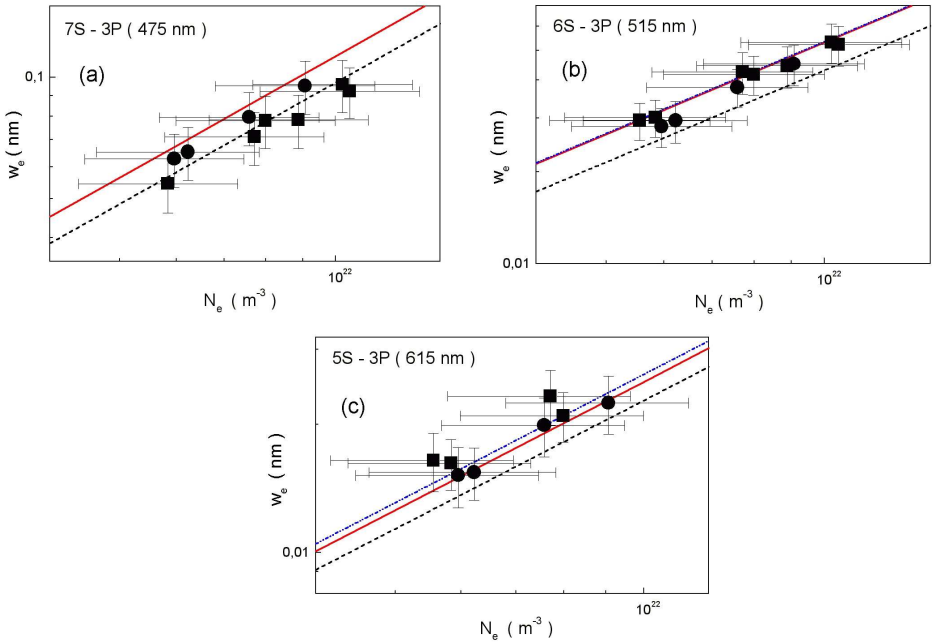

Fig. 6. Results of measurements of the Stark widths. Explanation of the symbols: filled squares - this experiment NaHg *discharge; filled circles - this experiment* NaCd *discharge; dashed line - theory [9]; solid line - theory [7]; The results are given: a) for the* 7S–3P *transition, b) for the* 6S–3P *transition; this panel also includes the results of calculations of Griem [8] (dot-dashed line) which practically coincide with the results of Dimitrijević [9], and c) for the* 5S–3P *transition; this panel also includes the results of calculations of Griem [8] (dot-dashed line). Estimated experimental error is* $\pm 25\%$*. Claimed uncertainty of calculated shifts is about 30% [7].*

In Figs. 7a – b, results of our measurements of line shifts of the 6D–3P and 5D–3P lines are compared with the available theoretical [7–9] and experimental data [11]. In the case of the 6D–3P transition, our experimental data are situated closely to the calculations of Refs. [7] and [11], and far away from the results given in Ref. [9]. In this case, our data are grouping together with the experimental data given in Ref. [11]. In the case of the 5D–3P transition, both calculations of Ref. [7] and Ref. [9] are within our experimental error bars ($\pm 25\%$), but one should also take into account that claimed uncertainty of the calculated shift data is about 30% [7]. Apparently, our data are grouping along the RPA theoretical results of Refs. [11] and [9]. While the estimated contribution of the ion broadening to the total line width and shift of the n^2S–3^2P lines is less than our estimated error ($\pm 25\%$), contribution of ion broadening to the total line width and shift of the n^2D–3^2P lines could be comparable to our error bars. Furthermore, for all nS–3P lines, the departure from isolated line approximation can be expected at very high electron densities $N_l \geq 1 \times 10^{23}\,\mathrm{m}^{-3}$, whereas this critical density for the 5D–3P line is about

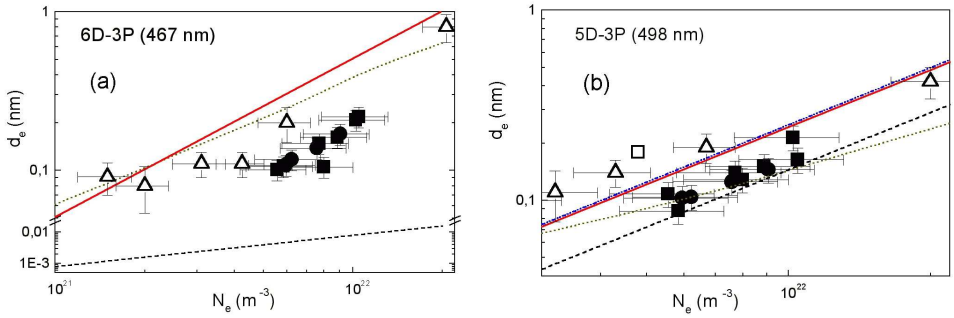

Fig. 7. Results of measurements of the Stark shifts. Explanation of the symbols: filled squares - this experiment NaHg *discharge; filled circles - this experiment* NaCd *discharge; open triangles - experiment [11]; dashed line - theory [9]; solid line - theory [7]; dotted line - RPA-theory [11]. The results are given: a) for the* 6D–3P *transition, b) for the* 5D–3P *transition; this panel also includes experimental result of Ref. [10] (open square) and the results of calculations of Griem [8] (dot-dashed line). Our estimated experimental error is* $\pm 25\%$*. Claimed uncertainty of calculated shifts is about 30% [7].*

$1 \times 10^{22}\,\mathrm{m}^{-3}$. For the 6D–3P line, the critical density is even lower, $4 \times 10^{21}\,\mathrm{m}^{-3}$, suggesting that these two lines could not be safely regarded as completely isolated.

Finally, in Fig. 8 the measured and theoretical Stark shifts of the sodium nS–3P lines ($n = 5, 6, 7$) at $N_\mathrm{e} = 1 \times 10^{22}\,\mathrm{m}^{-3}$ are plotted versus the upper-state quantum

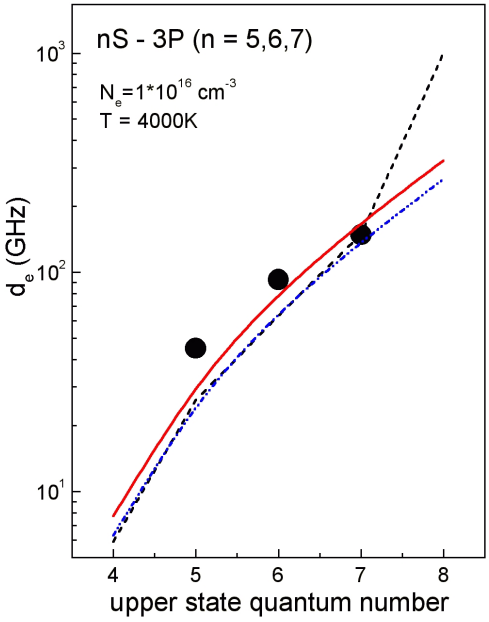

Fig. 8. Measured and calculated Stark shifts of sodium nS–3P lines ($n = 5, 6, 7$) at $N_\mathrm{e} = 1 \times 10^{16}\,\mathrm{cm}^{-3}$ plotted versus the upper-state quantum number. Note a systematic disagreement of the experiment and calculations for smaller quantum numbers ($n = 4, 5$), and also substantial disagreement of the theoretical data in the range of higher quantum numbers, $n \leq 8$. Explanation of the symbols: filled circles this experiment , dashed line - theory [9], solid line - theory [7], dot-dashed line - theory [8].

number. There is a smooth dependence of Stark shifts, both experimental and theoretical, on the upper-state quantum number up to the quantum number $n = 7$. The experimental data show a small systematic disagreement with the theoretical curves for smaller quantum numbers, but calculations disagree with the experiment substantially in the range of higher quantum numbers (with $n \geq 8$). Additional experiments are needed to clarify noted discrepancies.

6. *Conclusion*

We measured the Stark shifts and widths of neutral sodium spectral lines corresponding to n^2S–3^2P ($n = 5, 6, 7$) and m^2D–3^2P ($m = 5, 6$) transitions. The measurements are compared with the available theoretical [7–9, 11] as well as experimental data [11]. The 7S–3P line has been used as a calibration line to measure the electron density in both, NaHg and NaCd, high-pressure discharges. The data measured for the 6S–3P and the 5S–3P lines show a small but systematic discrepancy between experiment and theory. The line shifts of 5D–3P transition are in very good agreement with the available experimental and theoretical data. In the case of the 6D–3P transition, our experimental data are in a satisfactory agreement with the existing experimental and theoretical data. The residual discrepancies between experiment and theory can be attributed to the influence of ion broadening and, in the case of the nD–3P transitions, to the breakdown of the isolated-line approximation. In addition, the systematic disagreement between theory and experiment for smaller quantum numbers and substantial disagreement of calculations in the range of higher quantum numbers require additional experiments and calculations in order to clarify the noted disagreement.

Acknowledgements

We gratefully acknowledge the financial support from the Ministry of Science and Technology of the Republic of Croatia (project MZT 0119253), the partial financial support from the European Co-operation in the field of Scientific and Technical Research (COST Project 529) "Light Sources for the 21$^{\text{st}}$ Century" and the partial financial support from the joint USA-Croatia project JF107 (NIST) "Atomic Data for Optimisation of Light Sources".

References

[1] K. Schmidt, *Proc. 6th Int. Conf. Ion Phenomena in Gases 3*, Paris (1963) p. 323.

[2] J. J. de Groot and J. A. J. M. van Vliet, *The High-Pressure Sodium Lamp*, Philips Technical Library, Deventer (1986).

[3] G. Pichler, D. Fijan, D. Veža, J. Rukavina and J. Schlejen, Chem. Phys. Lett. **147** (1988) 497.

[4] G. Pichler, D. Veža and D. Fijan, Opt. Commun. **67** (1988) 45.

[5] D. Azinović, J. Rukavina, G. Pichler and D. Veža, Fizika (Zagreb) **22** (1989) 469.

[6] M. Born, J. Phys. D: Appl. Phys. **32** (1999) 2492.

[7] H. R. Griem, *Plasma Spectroscopy*, McGraw-Hill, New York (1964).

[8] H. R. Griem, *Spectral Line Broadening by Plasmas*, Academic Press, New York (1974).

[9] M. S. Dimitrijević and S. Sahal-Bréchot, J. Quant. Rad. Trans. **34** (1985) 149.

[10] W. J. van den Hoek and J. A. Visser, J. Phys. D: Appl. Phys. **14** (1981) 1613.

[11] M. Kettlitz and P. Oltmanns, Phys. Rev. E **54** (1996) 6741.

[12] H. Bartels, Z. Phys. **128** (1950) 546.

[13] H. P. Stormberg, J. Appl. Phys. **51** (1980) 1963.

[14] G. Traving, in *Plasma Diagnostics*, ed. W. Lochte-Holtgreven, North-Holland, Amsterdam (1968).

[15] D. Goebel and U. Hohm, Phys. Rev. A **52** (1995) 3691.

[16] D. Goebel and U. Hohm, J. Phys. Chem. **100** (1996) 7710.

[17] J. R. Fuhr and W. L. Wiese, in *CRC Handbook of Chemistry and Physics*, CRC Press, Boca Raton (1996).

[18] J. F. Kielkopf, J. F. Davies and J. A. Gwinn, J. Chem. Phys. **53** (1970) 2605.

[19] A. K. Hui, B. H. Armstrong and A. A. Wray, J. Quant. Spec. Rad. Trans. **19** (1978) 509.

[20] H. Margenau, Phys. Rev. **48** (1935) 755.

[21] W. R. Hindmarsh and J. M. Farr, J. Phys. B **2** (1969) 1388.

[22] H. P. Stormberg and R. Schaefer, J. Appl. Phys. **54** (1983) 4338.

[23] R. Schaefer and H. P. Stromberg, J. Appl. Phys. **57** (1985) 2512.

[24] H. Skenderović and V. Vujnović, J. Quant. Spec. Rad. Trans. **55** (1996) 155.

[25] H. Zwicker, in *Plasma Diagnostics*, ed. W. Lochte-Holtgreven, North-Holland, Amsterdam (1968).

[26] D. Balković, Diploma work (in Croatian), University of Zagreb (2002).

[27] W. H. Press, S. A. Teukolsky, W. T. Vetterling and B. P. Flannery, *Numerical recipes in C* (§13), Cambridge UP, New York (1995).

POMACI I ŠIRENJE NATRIJEVIH PRIJELAZA nS–3P I mD–3P U VISOKOTLAČNIM IZBOJIMA U NaCd I NaHg

Izvješćujemo o mjerenjima Starkovih pomaka i širina natrijevih spektralnih linija za prijelaze $n^2\mathrm{S}_{1/2} - 3^2\mathrm{P}_{3/2,1/2}$ ($n = 5, 6, 7$) i $m^2\mathrm{D}_{5/2,3/2} - 3^2\mathrm{P}_{3/2,1/2}$ ($m = 5, 6$). Mjerenja smo načinili za visokotlačne izboje Na-Hg-Xe i Na-Cd-Xe napajane izmjeničnom strujom. Starkov pomak natrijeve linije $7^2\mathrm{S}_{1/2} - 3^2\mathrm{P}_{1/2,3/2}$ služio je za određivanje elektronske gustoće. Usporedbom izračunatih i opažanih profila linija atomalnog natrija, određivali smo elektronske temperature i gustoće neutralnih čestica. Elektronska je gustoća iznosila 6×10^{21} do $1 \times 10^{22}\,\mathrm{m}^{-3}$ a temperatura između 3800 i 4100 K. Istraživali smo ovisnost mjerenih Starkovih pomaka i širina o elektronskoj gustoći i temperaturi. Ishode mjerenja usporedili smo s dostupnim teorijskim i ranijim eksperimentalnim podacima.